Dynamical friction in dark matter spikes: Corrections to Chandrasekhar's formula

Fani Dosopoulou*

School of Physics and Astronomy, Cardiff University, Cardiff, CF24 3AA, United Kingdom; Princeton Center for Theoretical Science, Princeton University, Princeton, New Jersey 08544, USA; and Department of Astrophysical Sciences, Princeton University, Princeton, New Jersey 08544, USA

(Received 26 May 2023; accepted 13 September 2024; published 15 October 2024)

We consider the intermediate mass-ratio inspiral of a stellar-mass compact object with an intermediate-mass black hole that is surrounded by a dark matter density spike. The interaction of the inspiraling black hole with the dark matter particles in the spike leads to dynamical friction. This can alter the dynamics of the black hole binary, leaving an imprint on the gravitational wave signal. Previous calculations did not include in the evaluation of the dynamical friction coefficient the contribution from particles that move faster than the inspiraling black hole. This term is neglected in the standard Chandrasekhar treatment where only slower moving particles contribute to the decelerating drag. Here, we demonstrate that dynamical friction produced by the fast moving particles can have a significant effect on the evolution of a massive binary within a dark matter spike. For a density profile $\rho \propto r^{-\gamma}$ with $\gamma \lesssim 1$, the dephasing of the gravitational waveform can be several orders of magnitude larger than estimated using the standard treatment. As γ approaches 0.5 the error becomes arbitrarily large. Finally, we show that dynamical friction tends to make the orbit more eccentric for any $\gamma < 1.8$. However, energy loss by gravitational wave radiation is expected to dominate the inspiral, leading to orbital circularization in most cases.

DOI: 10.1103/PhysRevD.110.083027

I. INTRODUCTION

The inspiral of an intermediate mass black hole (IMBH) and a solar mass type object will be observable by space-based gravitational wave (GW) detectors such as the Laser Interferometer Space Antenna (LISA) [1–4]. Around these IMBHs, a dark matter (DM) halo could grow adiabatically into a DM spike [5,6]. These spikes have extremely high densities and can leave an imprint on the GW signal emitted by the binary by modifying its orbital evolution. This opens up the possibility to infer the existence and the properties of the DM spike from measuring its impact on the GW signal [7,8].

The predicted effect is a dephasing of the gravitational waveform due to dynamical friction the secondary object experiences while passing through the mini spike. This decelerates the secondary object and results in a faster inspiral, which would be observable in the phase evolution of the GW signal [e.g., 9–14].

The dynamical friction force on the massive binary is calculated in the literature following the standard formulation of Chandrasekhar [15,16]. This has been also somewhat modified to include the back reaction of the DM spike to the binary motion [13], which is expected to flatten the inner cusp [e.g., 17,18]; the inclusion of relativistic terms in the treatment of the orbital dynamics and distribution of DM [19,20]; and DM accretion into the small compact object [10,11].

The calculation of the coefficient of dynamical friction is done by assuming that only DM particles that move slower than the inspiraling object contribute to the decelerating force. This corresponds to Chandrasekhar's result that stars moving faster than an inspiraling object have a negligible contribution to dynamical friction [15,21]. However, this approximation has been shown to break down when the gravitational potential around the binary is nearly Keplerian, as it is the case under consideration. [22,23] showed that in a cusp where the density falls off more slowly than $\rho \propto r^{-1}$, the contribution of the fast-moving particles to the fictional force becomes dominant and cannot be neglected.

In this work, we present a proof-of-concept analysis of the evolution of a massive binary in a DM cusp. For the first time, we include the dynamical friction force due to DM particles moving faster than an inspiraling black hole (BH). We compare to the standard treatment, and quantify the error made when this term is neglected.

We begin in Sec. II by introducing our formulation, including the orbit-averaged equations that describe the binary evolution due to dynamical friction and energy loss

*Contact author: dosopoulouf@cardiff.ac.uk

due to GW radiation. In Sec. III we explore the effect of the additional dynamical friction term on the orbital decay time of the binary, the evolution of its eccentricity, and study their dependence on the density profile slope of the DM spike. Finally, in Sec. IV we study the effect on the dephasing of the GW signal emitted by the binary. In Sec. V we summarize our main results and conclude.

II. FORMULATION

The general formula for the dynamical friction force a BH experiences during its inspiral inside a DM cusp is [22,23]

$$\boldsymbol{F}_{df} \approx -4\pi G^2 m\rho(r)\frac{\boldsymbol{v}}{v^3}\times\left\{\ln\Lambda\int_0^{v} dv_{\rm DM}4\pi f(v_{\rm DM})v_{\rm DM}^2 + \int_{v}^{v_{\rm esc}} dv_{\rm DM}4\pi f(v_{\rm DM})v_{\rm DM}^2\left[\ln\left(\frac{v_{\rm DM}+v}{v_{\rm DM}-v}\right) - 2\frac{v}{v_{\rm DM}}\right]\right\} \quad (1)$$

where $\boldsymbol{v}$ is the velocity of the inspiraling BH and m its mass; $\rho(r)$ is the local density of the DM particles, $f(v) = (1/n_M)d^6N/d^3xd^3v$ with $n_M = d^3N/d^3x$ is the normalized phase distribution (assumed to be isotropic), and $v_{\rm esc}$ is the escape velocity. The quantity $\ln\Lambda$ is the Coulomb logarithm defined as

$$\ln\Lambda = \ln\left(\frac{b_{\rm max}}{b_{\rm min}}\right) \approx \ln\left(\frac{b_{\rm max}v_c^2}{Gm}\right) \quad (2)$$

where $b_{\rm max}$ and $b_{\rm min}$ are the maximum and minimum impact parameters respectively and $v_c^2 = GM_\bullet/r$ the circular velocity around the IMBH of mass $M_\bullet$. The first integral term in the right-hand side (rhs) of Eq. (1) represents the decelerating drag due to DM particles moving slower than the infalling BH. The second integral term instead, represents the contribution from particles moving *faster* than the BH. This latter term is often neglected because it is typically a factor $\sim\ln\Lambda$ smaller than the former term. But, we will show below that under some specific conditions about the surrounding DM density profile and kinematics, the fast particle contribution becomes dominant.

We can rewrite the dynamical friction force as

$$\mathbf{F}_{df} = \epsilon(r,v)\frac{\boldsymbol{v}}{v^3} \quad (3)$$

where we defined

$$\epsilon(r,v) = -4\pi G^2\rho(r)m[\ln\Lambda\,\alpha(v) + \beta(v) + \delta(v)] \quad (4)$$

$$\alpha(v) = 4\pi\int_0^{v} f(v_{\rm DM})v_{\rm DM}^2 dv_{\rm DM} \quad (5)$$

$$\beta(v) = 4\pi\int_{v}^{v_{\rm esc}} f(v_{\rm DM})v_{\rm DM}^2\left[\ln\left(\frac{v_{\rm DM}+v}{v_{\rm DM}-v}\right)\right]dv_{\rm DM} \quad (6)$$

$$\delta(v) = 4\pi v\int_{v}^{v_{\rm esc}} f(v_{\rm DM})(-2v_{\rm DM})dv_{\rm DM}. \quad (7)$$

The osculating orbital element time-evolution equations of the inspiraling BH inside the DM cusp surrounding the IMBH due to dynamical friction are [23]

$$\frac{da}{dt} = \frac{2\epsilon(r,v)}{n^3a^2}\frac{(1-e^2)^{1/2}}{(1+e^2+2e\cos f)^{1/2}} \quad (8)$$

$$\frac{de}{dt} = \frac{2\epsilon(r,v)}{n^3a^3}(1-e^2)^{3/2}\frac{e+\cos f}{(1+e^2+2e\cos f)^{3/2}} \quad (9)$$

$$\frac{d\omega}{dt} = \frac{2\epsilon(r,v)}{n^3a^3}\frac{(1-e^2)^{3/2}}{(1+e^2+2e\cos f)^{3/2}}\frac{\sin f}{e} \quad (10)$$

$$\frac{df}{dt} = \frac{n(1+e\cos f)^2}{(1-e^2)^{3/2}} - \frac{d\omega}{dt} - \cos i\frac{d\Omega}{dt}. \quad (11)$$

where a is the semi-major axis, e the eccentricity, ω the argument of periapsis, Ω the longitude of the ascending node and f the true anomaly. $M = m + M_\bullet$ is the total binary mass and $n = 2\pi/T = (GM/a^3)^{1/2}$ the orbital angular frequency. We note that the perturbation of the binary orbit in this case is caused only by dynamical friction. Since there is no vertical component of the dynamical friction force to the orbital plane, the inclination i and the longitude of the ascending node Ω remains constant in the absence of other perturbing forces and thus $\dot{i} = \dot{\Omega} = 0$. Dynamical friction, however, induces a precession to the argument of periapsis, ω, and changes the orbital semimajor axis a and eccentricity e. This latter can either increase or decrease depending on the density profile slope of the DM spike adopted.

Since the time evolution of the orbital elements occur over many orbits, in order to determine the time evolution of the massive binary orbit we can orbit-average the above equations. In order to orbit-average a quantity along the orbit, we need to know how the true anomaly is changing over time. This is described by Eq. (11), which shows that apart from the unperturbed Keplerian evolution described by the first term on the rhs of Eq. (11), the true anomaly can also evolve due to possible precessions and specifically the periapsis precession $\dot{\omega}$ and the longitude of the ascending node precession $\dot{\Omega}$. Given that due to dynamical friction we have $\dot{\omega} \ll 1$ and that $\dot{\Omega} = 0$, we can compute the secular evolution of the orbital elements neglecting the second and third term in Eq. (11) and use

$$df = n\frac{(1+e\cos f)^2}{(1-e^2)^{3/2}}dt. \tag{12}$$

Under these considerations, the secular time-evolution equations of the binary orbit are

$$\left\langle \frac{da}{dt}\right\rangle_{\rm DF} = \frac{(1-e^2)^2}{\pi n^3 a^2}\int_0^{2\pi}\frac{(1+e\cos f)^{-2}\epsilon(r,v)}{(1+e^2+2e\cos f)^{1/2}}df \tag{13}$$

$$\left\langle \frac{de}{dt}\right\rangle_{\rm DF} = \frac{(1-e^2)^3}{\pi n^3 a^3} \times \int_0^{2\pi}\frac{(e+\cos f)\epsilon(r,v)}{(1+e^2+2e\cos f)^{3/2}(1+e\cos f)^2}df, \tag{14}$$

$$\left\langle \frac{d\omega}{dt}\right\rangle_{\rm DF} = 0. \tag{15}$$

Thus, over many orbits dynamical friction will change the semi-major axis and eccentricity of the orbit but on average it will cause no in-plane precession of the orbit.

Below a certain distance between the two BHs, energy loss by GWs becomes important and needs to be added to the dynamical friction effect. This is certainly the case for a massive binary in the LISA frequency band 0.1 mHz–1 Hz. The orbital evolution due to GW energy loss is [24]

$$\left\langle \frac{da}{dt}\right\rangle_{\rm GW} = -\frac{64G^3 m M_\bullet (m+M_\bullet)}{5c^5 a^3(1-e^2)^{7/2}}f_1(e) \tag{16}$$

$$\left\langle \frac{de}{dt}\right\rangle_{\rm GW} = -\frac{304G^3 m M_\bullet (m+M_\bullet)}{15c^5 a^4(1-e^2)^{5/2}}f_2(e) \tag{17}$$

where the eccentricity dependent terms are $f_1 = 1+\frac{73}{24}e^2+\frac{37}{96}e^4$ and $f_2 = 1+\frac{121}{204}e^4$.

Finally, we obtain the evolution of the inspiraling BH orbit by integrating the following coupled set of first order differential equations

$$\left\langle \frac{da}{dt}\right\rangle = \left\langle \frac{da}{dt}\right\rangle_{\rm DF} + \left\langle \frac{da}{dt}\right\rangle_{\rm GW} \tag{18}$$

$$\left\langle \frac{de}{dt}\right\rangle = \left\langle \frac{de}{dt}\right\rangle_{\rm DF} + \left\langle \frac{de}{dt}\right\rangle_{\rm GW}. \tag{19}$$

III. EFFECT ON THE BINARY ORBIT

We consider here the simple case in which the DM cusp is a power law profile

$$\rho(r) \propto r^{-\gamma}. \tag{20}$$

Assuming that the gravitational potential Φ is dominated by the central IMBH and neglecting the effect of the surrounding DM particles we can write $\Phi \approx -GM_\bullet/r$. Eddington's formula then uniquely leads to the following distribution function of the DM particle velocities [25]

$$f(v_{\rm DM}) = \frac{\Gamma(\gamma+1)}{\Gamma(\gamma-\frac{1}{2})}\frac{1}{2^\gamma \pi^{3/2} v_c^{2\gamma}}(2v_c^2 - v_{\rm DM}^2)^{\gamma-3/2} \tag{21}$$

where the normalization corresponds to unit total number. We employ the distribution function to calculate the effect of dynamical friction on the orbit of the inspiraling BH.

We consider a binary with primary IMBH mass $M_\bullet = 1.4\times10^3 M_\odot$, mass ratio $q = m/M_\bullet = 10^{-3}$, initial $a_0 = 10^{-8}$ pc and $e_0 = 0.1$. Based on these initial conditions, the binary is intially in the LISA frequency band, 0.1 mHz–1 Hz, with a small but finite eccentricity. We evaluate the importance of dynamical friction on the evolution of the binary a and e, and comment on the effect of the "nondominant" terms.

Figure 1 shows the quantity $\mathcal{R} = \frac{1}{e}\langle\dot{e}\rangle_{\rm DF}/\frac{1}{a}\langle\dot{a}\rangle_{\rm DF}$ as a function of γ; $\mathcal{R}$ represents an approximation of the fractional change in eccentricity in a time $a/\langle\dot{a}\rangle_{\rm DF}$, i.e., the orbital decay timescale due to dynamical friction. For $\mathcal{R}<0$ the orbit becomes more eccentric, for $\mathcal{R}>0$ it circularizes, and for $\mathcal{R}=0$ the eccentricity remains constant. From the value of $\mathcal{R}$, we expect dynamical friction to have a small effect on the evolution of the binary's eccentricity. The evolution remains dominated by GW

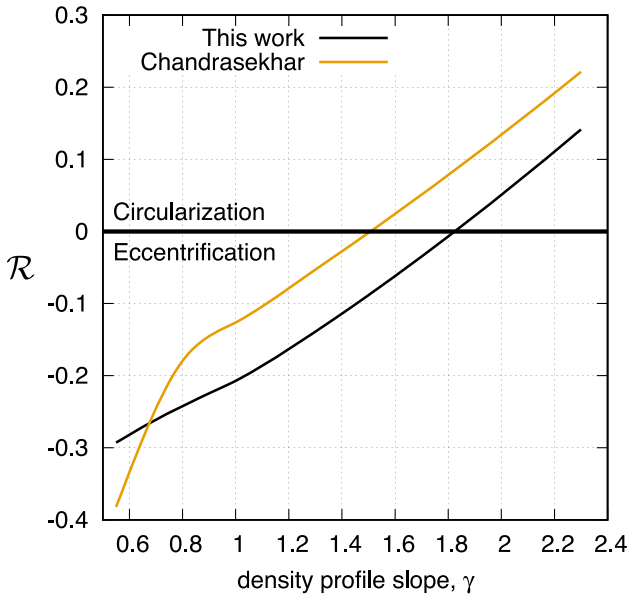

FIG. 1. Evolution of eccentricity due to dynamical friction, including the contribution form the fast moving particles. In cusps with $\gamma > 1.8$, dynamical firction causes the orbit to circularize faster than if it was evolved only due to energy loss by GW radiation. For shallower slopes, instead, the orbit is expected to circularize at a slower rate. Note that in the standard treatment of Chandrasekhar, the transition occurs at $\gamma = 1.5$. In this calculation we did not include the 2.5 pN terms that are always dominant and cause the orbit to circularize.

energy loss, which leads to the circularization of the binary. This conclusion is in contrast to what stated in [26], who finds that generally the binary becomes more eccentric. [27] find that by including the relative velocities of the DM particles, dynamical friction tends to circularize the orbit. We agree with the latter authors, but find that dynamical friction tends to circularize the orbit for a smaller range of density profile slopes. Using our more complete formulation, we find that the effect is to circularize the orbit for any $\gamma \gtrsim 1.8$. Instead, the standard Chandrasekhar's treatment predicts orbital circularization for any $\gamma \gtrsim 1.5$ [28].

Reference [27] shows that at first order $(a/e)(de/da) = \gamma/2$ when dynamical friction is the dominant form of energy loss and in the limit of slow-moving particles, demonstrating that DM effects can be observable not just from dephasing but also from the circularization rate. Our results agree with this conclusion, but require a modification of the binary orbit circularization rate due to the fast moving particles.

Figure 2 further quantifies the deviation from Chandrasekhar's treatment as a function of the power law index of the density profile. We compute the relative error that one would make by using the standard Chandrasekhar's formula compared to our treatment. This is obtained as $\Delta_a = \frac{|T_{\rm C;a} - T_{\rm df;a}|}{T_{\rm df;a}}$, and $\Delta_e = \frac{|T_{\rm C;e} - T_{\rm df;e}|}{T_{\rm df;e}}$ where

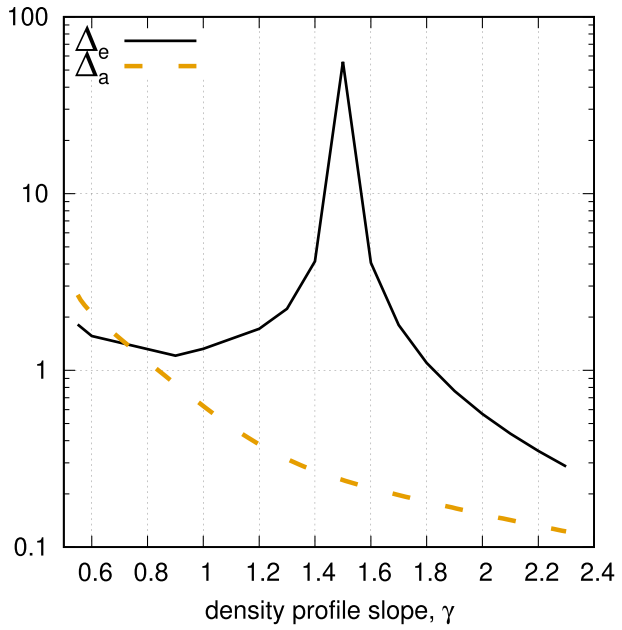

FIG. 2. Relative error in the dynamical friction evolution timescale made when neglecting the contribution from the fast moving particles. We plot $\Delta_a = \frac{|T_{\rm C;a} - T_{\rm df;a}|}{T_{\rm df;a}}$ and $\Delta_e = \frac{|T_{\rm C;e} - T_{\rm df;e}|}{T_{\rm df;e}}$, as defined in the main text, as a function of the density profile slope. For $\gamma < 0.8$, the standard formula predicts an orbital decay time that is more than twice as long than predicted by our treatment. Deviations in e is significant for any value of γ. For $\gamma = 2$, our treatment predicts a circularization timescale that is about 2 times shorter than the standard formula.

$$T_{\rm df;a} = \frac{a}{|\langle \dot{a} \rangle_{\rm DF}|}; \tag{22}$$

is the orbital decay timescale, and

$$T_{\rm df;e} = \frac{e}{|\langle \dot{e} \rangle_{\rm DF}|}; \tag{23}$$

is the timescale of eccentricity evolution. $T_{\rm C;a}$ and $T_{\rm C;e}$ are the dynamical friction timescales for orbital decay and eccentricity evolution obtained from the standard Chandrasekhar's formula, respectively.

From this analysis, we can see that the contribution from the fast moving particles on the evolution of a becomes more important as γ approaches 0.5 from above. For $\gamma < 0.8$, the standard formula predicts an orbital decay time that is more than twice as long than predicted by the our treatment. The contribution from the fast moving particles has also an effect on e. Deviations in this case remains significant for essentially any value of γ. For $\gamma = 2$, our treatment predicts a circularization timescale that is about 2 times shorter than the standard formula.

IV. EFFECT ON THE WAVEFORM: DEPHASING

To quantify the size of the dephasing effect due to dynamical friction, we estimate the difference between the number of gravitational wave cycles during the inspiral in vacuum and in presence of a DM minispike, for various density profile models. We calculate this for models where the contribution of fast moving particles is neglected as in the literature, and in models that include the effect of the fast particles.

We define the number of GW cycles by integrating the GW frequency between two times

$$N_{\rm c} = \int_{t_1}^{t_2} f_{\rm GW}(t) dt. \tag{24}$$

In the approximation where the binary is circular, the GW frequency is twice the orbital frequency. Eccentric binaries emit a GW signal with a broad spectrum of frequencies; the peak gravitational wave frequency corresponding to the harmonic which leads to the maximal emission of GW radiation can be approximated as [29]

$$f_{\rm GW,peak} = \frac{\sqrt{GM}}{\pi} \frac{1+e}{[a(1-e^2)]^{3/2}}, \tag{25}$$

and its time evolution is obtained from the evolution of a and e calculated from Eqs. (18) and (19).

The difference in the number of GW cycles with and without DM, is then defined as

$$\Delta N_{\rm c} = N_{\rm c}^{\rm vacum} - N_{\rm c}^{\rm DM}. \tag{26}$$

We assume that the central IMBH is surrounded by a DM spike, formed as a consequence of the adiabatic growth of the central IMBH in a DM halo. After its formation, the central density of the DM spike is likely to be lowered by several processes, which include the perturbative effect of inspiraling BHs [13] and/or DM self-annihilation [30–34]. We note that the profile of the DM spike depends on the formation history of the central IMBH. If the IMBH has experienced disruptive processes such as mergers in the past, the minispike would be weakened or even disappear [7,8]. Furthermore, self annihilations cause the DM density to decay which can result in a weak density plateau, $\propto r^{-0.5}$, near the SMBH [30–34]. For the above reasons the slope of a power law DM spike profile $\rho_{\rm sp}(r) \propto r^{-\gamma}$ can be essentially treated as a free parameter within the range $0 \lesssim \gamma \lesssim 3$ [7,8].

Correspondingly, we model the DM spike using a broken power law model:

$$\rho(r) = \begin{cases} \rho_0 \left(\frac{r}{r_0}\right)^{-\gamma} \left[1 + \left(\frac{r}{r_0}\right)^{\alpha}\right]^{(\gamma-\gamma_e)/\alpha}, & \text{if } r > r_{\rm in} \\ 0, & \text{if } r \le r_{\rm in} \end{cases} \tag{27}$$

where ρ_0 is the density normalization, $r_{\rm in} = 4GM_\bullet/c^2$ is the innermost stable circular orbit radius and α is a parameter that defines the transition strength between an inner power law cusp with slope γ and the outer power law profile with slope γ_e. The scale r_0 is the radius where this transition occurs.

The normalization of the density profile is chosen such that the density at infinity matches that of the density model in [7,8]

$$\rho_{\rm sp}(r) = \rho_{\rm sp} \left(\frac{r}{r_{\rm sp}}\right)^{-\gamma_e} \tag{28}$$

where

$$r_{\rm sp} \approx \left[\frac{(3-\gamma_e) 0.2^{3-\gamma_e} M_\bullet}{2\pi\rho_{\rm sp}}\right]^{1/3}. \tag{29}$$

and $\rho_{\rm sp}$ is the density normalization chosen to be $\rho_{\rm sp} = 226 M_\odot\,{\rm pc}^{-3}$ [13]. This model is the fiducial model investigated in [7,8]. The slope $\gamma_{\rm e} = 7/3$ is expected to develop in the center of a halo with an initial profile scaling $\rho \sim r^{-1}$, such as an NFW profile. For this reason, we set $\gamma_{\rm e} = 7/3$ and explore the dependence of our results on the assumed value of the inner slope γ, which we take to be 0.55, 0.8 and 1. We set the break radius $r_0 = 3 \times 10^{-8}$ pc, so that for the assumed initial galactocentric radius, $a_0 = 2 \times 10^{-8}$ pc, the inspiral is completely within the core, where the dynamical friction effect is maximized. We set $\alpha = 5$ that corresponds to a sharp transition. For any $\alpha \gtrsim 5$ our results remain essentially unchanged. However, as α is lowered the effect of the fast moving stars is somewhat reduced due to the models being more similar to the single power-law $\gamma_e = 2.3$ model over a wider range of radii.

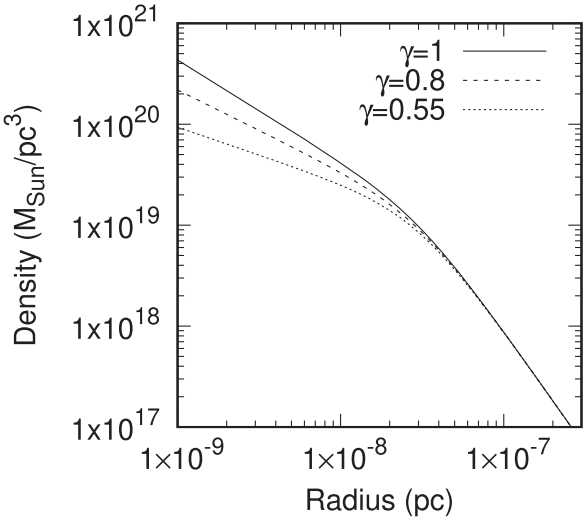

FIG. 3. Dark matter spike density profile models corresponding to the density used in this work (Eq. 27), for different values of inner power law slope γ. Solid line is for $\gamma = 1$, dashed line for $\gamma = 0.8$ and dotted line for $\gamma = 0.55$. The models are normalized such to have the same density at infinity.

We show the density profile models in Fig. 3. We note that our choice of normalization is different with what often used in the literature. For example, [13] use the model of Eq. (28), and vary γ_e across a range of values. Given this choice, shallower profiles mean a much smaller central density. The result is that the effect of dynamical friction rapidly becomes unimportant for $\gamma_e \le 3/2$. Thus, the decreasing dynamical friction in this case is not because of the change in γ_e, but because of the different normalization that leads to much lower central densities. On the other hand, our models all have the same normalization outside r_0, which keeps the density high inside this radius and dynamical friction important for most values of γ.

Generally, the distribution function $f(v_{\rm DM})$ corresponding to the density model in Eq. (27) and the potential generated by the DM and central IMBH cannot be obtained analytically. We therefore solve the Eddington equation numerically to obtain the distribution function and then compute numerically the integrals that appear in the rhs of Eq. (1). We note that the first of these integrals can be simplified using the following expression [22,35]:

$$F(<v,r) = \int_0^v dv_{\rm DM} 4\pi f(v_{\rm DM}) v_{\rm DM}^2 = 1 - \frac{1}{\rho}\int_0^E d\phi' \frac{d\rho}{d\phi'} \times \left\{1 + \frac{2}{\pi}\left[\frac{v/\sqrt{2}}{\sqrt{\phi'-E}} - \tan^{-1}\left(\frac{v/\sqrt{2}}{\sqrt{\phi'-E}}\right)\right]\right\}, \tag{30}$$

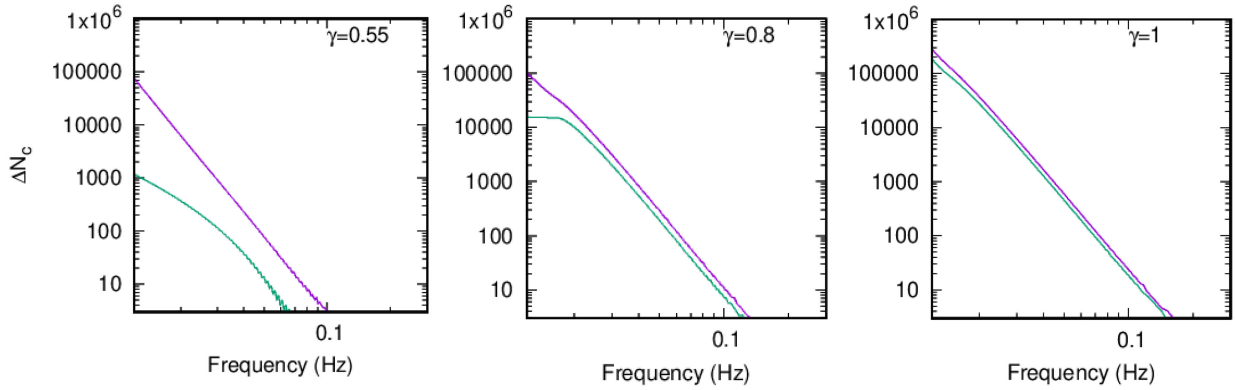

FIG. 4. Change in the number of GW cycles with respect to the vacuum inspiral. Purple lines are obtained from equations (18) and (19) that include the contribution from the fast moving particles. Green lines were obtained using the standard Chandrasekhar's formula.

where $E = \frac{1}{2}v^2 + \phi(r)$; $F(< v, r)$ is simply the fraction of DM particles at r that move slower than the infalling BH.

Since we are interested to show a proof-of-concept example in this work, we simply consider a single set of initial conditions. Moreover, we only consider circular orbits, and plan to look at eccentric orbits in a future work. As stated above, the initial semimajor axis of the orbit is $a_0 = 2 \times 10^{-8}$ pc, smaller than r_0. Thus, the binary effectively moves within a density spike of slope γ. As before, the primary BH mass is $M_\bullet = 1.4 \times 10^3 M_\odot$ and the binary mass ratio is $q = 10^{-3}$. Given these masses and the orbit, the binary GW frequency is $8.9 \times 10^{-3} Hz$; i.e., it is within the LISA frequency band 0.1 mHz–1 Hz. The orbit evolves completely within this frequency window until it reaches coalescence.

The results of our calculation are shown in Fig. 4. For $\gamma = 0.55$, we see that the dynamical friction contribution from the fast moving particles leads to nearly two orders of magnitude difference in the value of ΔN_c with respect to the standard treatment. The difference is larger at lower frequencies, but remains almost an order of magnitude throughout. As γ is increased, the relative contribution of the fast moving particles to dynamical friction decreases. It is still important for $\gamma = 0.8$ at $f \sim 10^{-2}$ Hz, but at higher frequencies and/or for larger γ the difference is small.

V. CONCLUSIONS

In this work we have considered the evolution of a massive binary inside a DM density spike. For the first time we included in the treatment of this problem, the dynamical friction produced by particles that move faster than the inspiraling BH, usually referred to as "nondominant" term. This term is neglected in the standard Chandrasekhar treatment where all the frictional force is assumed to be produced by particles moving slower than the binary. We have studied the effect of this term on the orbital decay, and on the circularization time of the binary. We then studied the dephasing of the gravitational waveform produced by the binary due to dynamical friction. Our main conclusions are summarized in what follows:

(1) The evolution of the binary eccentricity due to dynamical friction is shown to be significantly affected. The parameter space where dynamical friction causes the orbit to become more eccentric is enlarged when the contribution from the fast moving particles is included. In our treatment, dynamical friction leads the orbit to become more eccentric for any cusp with slope $\gamma < 1.8$, while the standard treatment would predict $\gamma < 1.5$ (Fig. 1). For $\gamma \gtrsim 1.8$, dynamical friction causes the orbit to circularize faster than if evolved only due to energy loss by GW radiation. For shallower slopes, instead, the orbit is expected to circularize at a slower rate (Fig. 1).

(2) The timescale over which the binary eccentricity evolves is also significantly modified by the nondominant terms. This statement appears to be true for most values of γ. For $\gamma = 2$, our treatment predicts a circularization timescale that is about 2 times shorter than the standard formula (Fig. 2).

(3) For $\gamma \leq 1$ the orbital decay time of the binary due to dynamical friction is much shorter than predicted by the Chandrasekhar's formula. For $\gamma = 1$ the difference is a factor of 2. But, as γ approaches 0.5, the error due to neglecting the fast moving particles becomes arbitrarily large (Fig. 2).

(4) We calculate the dephasing of the GW signal due to dynamical friction. We show that the dephasing of the gravitational waveform induced by DM can be much larger than previously thought. The difference between the dephasing computed with the standard treatment and ours can be as large as two orders of magnitude for $\gamma \lesssim 0.6$, while it likely to be negligible for any $\gamma \gtrsim 1$ (Fig. 4).

In this article we demonstrated that the dynamical friction from the fast moving particles can have a significant effect on the evolution of a massive binary within a DM spike. The effect is very sensitive to the slope of the

DM distribution, rapidly becoming important for $\gamma \lesssim 1$. Shallow density cusps can be produced, for example, by the interaction of the inspiraling BH with the surrounding cusp, or by DM self-annihilation. It is therefore our recommendation, that future similar studies will consider the replacement of the standard Chandrasekhar's formula with Eqs. (13) and (14).

Since we were interested in isolating the contribution of the fast moving DM paerticles to dynamical friction, we have based our models on a number of simplifying assumptions. We have assumed that the DM spike is not affected by the binary motion; we have assumed that the velocity distribution of the DM particles is isotropic; and we have ignored the possibility that DM is accreated directly onto the inspiraling BH. Moreover, our work does not take into account relativistic terms in the description of the orbital dynamics and distribution of DM. Although our assumptions are likely to break down in realistic situations, we expect that the fast moving particles will still play an important contribution to the dynamical friction force.

ACKNOWLEDGMENTS

This work is supported by the UK's Science and Technology Facilities Council Grant No. ST/V005618/1.

[1] P. Amaro-Seoane *et al.*, arXiv:1201.3621.
[2] P. Amaro-Seoane *et al.*, arXiv:1702.00786.
[3] P. Amaro-Seoane *et al.*, arXiv:1702.00786.
[4] E. Barausse, V. Cardoso, and P. Pani, Phys. Rev. D **89**, 104059 (2014).
[5] P. Gondolo and J. Silk, Phys. Rev. Lett. **83**, 1719 (1999).
[6] L. Sadeghian, F. Ferrer, and C. M. Will, Phys. Rev. D **88**, 063522 (2013).
[7] K. Eda, Y. Itoh, S. Kuroyanagi, and J. Silk, Phys. Rev. Lett. **110**, 221101 (2013).
[8] K. Eda, Y. Itoh, S. Kuroyanagi, and J. Silk, Phys. Rev. D **91**, 044045 (2015).
[9] X.-J. Yue and W.-B. Han, Phys. Rev. D **97**, 064003 (2018).
[10] C. F. B. Macedo, P. Pani, V. Cardoso, and L. C. B. Crispino, Astrophys. J. **774**, 48 (2013).
[11] X.-J. Yue, W.-B. Han, and X. Chen, Astrophys. J. **874**, 34 (2019).
[12] V. Cardoso and A. Maselli, Astron. Astrophys. **644**, A147 (2020).
[13] B. J. Kavanagh, D. A. Nichols, G. Bertone, and D. Gaggero, Phys. Rev. D **102**, 083006 (2020).
[14] N. Becker and L. Sagunski, Phys. Rev. D **107**, 083003 (2023).
[15] S. Chandrasekhar, Astrophys. J. **97**, 255 (1943).
[16] S. Chandrasekhar, Astrophys. J. **97**, 263 (1943).
[17] D. Merritt, S. Harfst, and G. Bertone, Phys. Rev. D **75**, 043517 (2007).
[18] F. Dosopoulou, J. E. Greene, and C.-P. Ma, Astrophys. J. **922**, 40 (2021).
[19] N. Speeney, A. Antonelli, V. Baibhav, and E. Berti, Phys. Rev. D **106**, 044027 (2022).
[20] C. Chiari and P. Di Cintio, Astron. Astrophys. **677**, A140 (2023).
[21] J. Binney and S. Tremaine, *Galactic Dynamics*, 2nd ed., edited by James Binney and Scott Tremaine (Princeton University Press, Princeton, NJ USA, 2008), ISBN 978-0-691-13026-2.
[22] F. Antonini and D. Merritt, Astrophys. J. **745**, 83 (2012).
[23] F. Dosopoulou and F. Antonini, Astrophys. J. **840**, 31 (2017).
[24] P. C. Peters, Phys. Rev. **136**, 1224 (1964).
[25] D. Merritt, *Dynamics and Evolution of Galactic Nuclei* (Princeton University Press, Princeton, 2013).
[26] V. Cardoso, C. F. B. Macedo, and R. Vicente, Phys. Rev. D **103**, 023015 (2021).
[27] N. Becker, L. Sagunski, L. Prinz, and S. Rastgoo, Phys. Rev. D **105**, 063029 (2022).
[28] A. Gould and A. C. Quillen, Astrophys. J. **592**, 935 (2003).
[29] L. Wen, Astrophys. J. **598**, 419 (2003).
[30] G. Bertone, Phys. Rev. D **73**, 103519 (2006).
[31] G. Bertone and D. Merritt, Phys. Rev. D **72**, 103502 (2005).
[32] G. Bertone and T. M. P. Tait, Nature (London) **562**, 51 (2018).
[33] E. Vasiliev, Phys. Rev. D **76**, 103532 (2007).
[34] D. Merritt, arXiv:1001.3706.
[35] D. Merritt and A. Szell, Astrophys. J. **648**, 890 (2006).